RESOLVING PHASE AMBIGUITY IN THE INVERSE PROBLEM OF REFLECTION-ONLY MEASUREMENT METHODS

U. C. Hasar[1, 2, *], J. J. Barroso[3], C. Sabah[4], and Y. Kaya[1]

[1]Department of Electrical and Electronics Engineering, Ataturk University, Erzurum 25240, Turkey

[2]Center for Research and Application of Nanoscience and Nanoengineering, Ataturk University, Erzurum 25240, Turkey

[3]Associated Plasma Laboratory, National Institute for Space Research, São José dos Campos, SP 12227-010, Brazil

[4]Physikalisches Institut, J. W. Goethe Universität, Frankfurt, Germany

Abstract—We have applied the phase unwrapping technique to resolve the phase ambiguity problem arising from complex expressions of scattering parameters, for reflection-only measurement configurations, since, at some instances, only one side of the sample under test is accessible for electromagnetic measurements. We considered two different measurement configurations for testing the applicability of the phase unwrapping technique as: 1) two identical samples with different lengths flushed by a short-circuit termination and 2) one sample shorted by a varying short-circuit termination. For each measurement configuration, the underlying expressions for the reflection scattering parameters are derived. For both cases, we evaluated the suitability of the phase unwrapping technique by considering a highly-dispersive medium (distilled water) as our test sample. We note that continuity of the real part of the complex wavelength is a key issue in the unwrapping technique for (one-port) reflection-only measurements.

1. INTRODUCTION

Transmission-reflection and reflection-only non-resonant methods have been widely utilized for characterization of materials owing to their

relative simplicity, broad frequency coverage, and higher accuracy [1–14]. There are few problems of these methods such as undesired ripples in the measured parameters, the increased uncertainty in reference-plane positions, and multiple solutions for electromagnetic parameters. Among these problems, multiple-solutions ambiguity, which is of our main concern in this study, arises from the effect of non-unique retrieval of the imaginary part of the complex propagation factor, T, in scattering (S-) parameter equations. A variety of techniques have been put forward for retrieving the correct solutions for ε_r and/or μ_r [15–27]. For example, multiple solutions problem can be avoided by choosing a material thickness less than one-quarter wavelength [15, 16]. However, thin materials can result in sagging, which alters the theoretical formulations, and also decrease the feasibility and repeatability of measurements. In [17], Weir proposed a technique that compares the calculated and measured group delays of the signal propagating through the sample, although this method might not be valid for highly dispersive media since the concept of group velocity is no longer useful in regions of anomalous dispersion. With regard to dielectric materials, a different approach [18–23] to the multivalued problem for the determination of the permittivity of low-loss or lossy samples relies on using transmission-only measurements at two close frequencies to estimate an accurate initial guess for the permittivity. Upon using the mathematical continuity of ε_r and μ_r parameters, an iterative method [24] determines the proper branch by verifying whether the candidate initial branch satisfies causality relations at each frequency step using at least two identical samples with different lengths. Furthermore, Buyukozturk et al. proposed a technique which uses time difference of arrival along with S_{21} measurements for overcoming the same problem [25].

Alternatively, based on the fact that the real part (attenuation factor) in the complex propagation is independent of the phase ambiguity, with only the determination of the imaginary part (phase factor) depending on the phase change, other works [26, 27] have enforced causality to calculate the phase factor from the attenuation factor. Such a method, however, requires that real part of the propagation factor be known as a function of frequency in the entire spectrum. Since this is not possible, the Kramers-Kronig relation is numerically integrated over a truncated frequency range thus providing an approximation for the phase factor.

Apart from these previously mentioned methods which deal in a limited way with the phase ambiguity problem, in a recent study, we have applied the phase unwrapping method to resolve the phase ambiguity in measured constitutive parameters of low-to-

high-loss materials for transmission-reflection (two-port) methods [28]. Simple and not relying on heavy computation as the Kramers-Kronig approach does, such a technique correctly retrieves the phase of the complex wavenumber by detecting successive phase jumps that exceed π at specific frequencies. The phase unwrapping method finds a variety of applications, for instance, in continuous-wave interferometry, holographic measurements by Fourier transform technique, computed tomography, digital phase demodulation techniques, medical imaging, and so on [29]. The physical quantities of interest are encoded in the phase of the complex signal and the unwrapping method allows extracting the information conveyed by the signal by correctly interpreting the ambiguity of the phase, which can only be derived as modulo 2π. In this research paper, we extend this powerful method to retrieve the constitutive parameters of materials using reflection-only (one-port) measurements because, in some instances, only one side of the specimen under test is visible to electromagnetic signals [30, 31], and because the use of the phase unwrapping method becomes a significant issue in characterization of materials, especially for highly-dispersive media, in which anomalous dispersion takes place as the one studied here (distilled water). Two typical reflection-only measurement scenarios are considered, and for each configuration, the necessary expressions for ε_r and μ_r are derived. We selected distilled water as a highly dispersive test specimen, and then uniquely and non-ambiguously retrieved its electromagnetic properties from the considered two different reflection-only measurement configurations.

2. EXPRESSIONS AND RETRIEVAL PROCEDURES

In this section, we first derive expressions of S-parameters of two reflection-only measurement configurations, and then present the retrieval process of ε_r and μ_r of samples for each configuration.

2.1. Two Identical Samples with Different Length

The retrieval problem of two identical samples with different lengths, L_1 and L_2 is pictured in Fig. 1. It is assumed that the sample is a simple medium (linear, homogeneous, and isotropic) and is placed inside an empty rectangular waveguide. In addition, we presume that the short-circuit termination is flushed (in contact) with the sample back surface at interface II-III, and that the calibration plane coincides with the front face of each sample in Fig. 1.

The expressions of electric and magnetic fields, $\vec{E}$ and $\vec{H}$, in each region in Fig. 1 can be derived from their vector potentials (or Hertzian
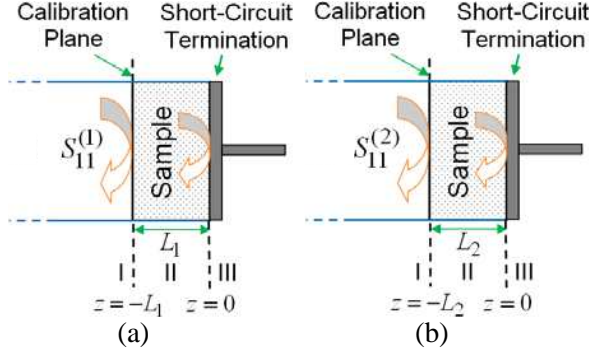
Figure 1. Measurement configuration for constitutive parameters retrieval from two-sample measurements through the phase unwrapping technique.

vectors), $\vec{A}$ and $\vec{F}$, as in [32]

$$
\vec{E} = -i\omega\vec{A} - i\frac{1}{\omega\mu\varepsilon}\nabla\left(\nabla \bullet \vec{A}\right) - \frac{1}{\varepsilon}\nabla \times \vec{F},
$$
$$
\vec{H} = \frac{1}{\mu}\nabla \times \vec{A} - i\omega\vec{F} - i\frac{1}{\omega\mu\varepsilon}\nabla\left(\nabla \bullet \vec{F}\right), \tag{1}
$$

where $\varepsilon = \varepsilon_0\varepsilon_r$ and $\mu = \mu_r\mu_0$. Here, ε_0 and μ_0 are the (absolute) permittivity and permeability of vacuum, and the time dependence of $\exp(i\omega t)$ is assumed in the phasor (complex) domain. Assuming that the rectangular waveguide operates in the dominant mode (TE_{10}^z), we have $\vec{A} = 0$, $F_x = 0 = F_y$ and $\partial F_z/\partial y = 0$ [32]. Then, the electric vector potential, $\vec{F}$, for regions I and II in Fig. 1 can be written

$$
F_z^{(I)}(x, z) = \psi(x)\left[C_1 e^{-\gamma_0 z} + C_2 e^{\gamma_0 z}\right],
$$
$$
F_z^{(II)}(x, z) = \psi(x)\left[C_3 e^{-\gamma z} + C_4 e^{\gamma z}\right], \tag{2}
$$

$$
\psi(x) = \cos\left(\frac{2\pi}{\lambda_c}x\right), \quad \gamma_0 = i\frac{2\pi}{\lambda_0}\sqrt{1 - \frac{\lambda_0^2}{\lambda_c^2}}, \quad \gamma = i\frac{2\pi}{\lambda_0}\sqrt{\varepsilon_r\mu_r - \frac{\lambda_0^2}{\lambda_c^2}}. \tag{3}
$$

Here, $C_1 : C_4$ are complex amplitudes; γ and γ_0 are the propagation constants inside the sample and air regions of the guide; $\lambda_0 = c/f$ and $\lambda_c = c/f_c$ correspond to the free-space and cut-off wavelengths; f, f_c, and c are the operating and cut-off frequencies and the speed of light, respectively; and $\varepsilon_r = \varepsilon_r' - i\varepsilon_r''$ and $\mu_r = \mu_r' - i\mu_r''$.

Using the electric vector potentials in Eq. (2), electric and magnetic fields can be determined from Eq. (1). Applying boundary conditions (continuation of tangential components of electric and

magnetic fields and vanishing of tangential electric field at the short-circuit termination (PEC)) at interfaces I-II and II-III ($z = 0$ and $z = -L_1$ or $z = -L_2$), reflection scattering parameter (S_{11}) at the calibration plane can be derived as

$$S_{11}^{(u)} = \frac{\Gamma - T_u^2}{1 - \Gamma T_u^2}, \quad \Gamma = \frac{\gamma_0 \mu_r - \gamma}{\gamma_0 \mu_r + \gamma}, \quad T_u = e^{-\gamma L_u}. \tag{4}$$

In Eq. (4), $u = 1, 2$; Γ is the first reflection coefficient at the interface I-II and T_1 and T_2 are the propagation factors of samples with lengths L_1 and L_2.

The well-known Nicolson-Ross-Weir technique [4, 17] cannot be applied to our problem, for it was devised for reflection-transmission (two-port) measurements. Following a similar procedure in [33] and from Eq. (4), we obtain a relation between T_1 and T_2

$$T_u^2 = \left(\Gamma - S_{11}^{(u)}\right) \Big/ \left(1 - \Gamma S_{11}^{(u)}\right), \ T_2^2 = \left(T_1^2\right)^k, \ k = L_2/L_1. \tag{5}$$

Utilizing an optimization technique for non-linear expressions, the accurate and unique value of Γ can be computed from Eq. (5), where $S_{11}^{(1)}$ and $S_{11}^{(2)}$ are known or measured quantities, and from the foregoing relation together with the constraint $|\Gamma| \leq 1$, corresponding to positive heat dissipation for passive samples [34–36]. But, for some specific combination of sample lengths, an analytical solution for Γ can be attained. For instance, for $k = 2$ ($L_2 = 2L_1$), we have

$$\Gamma_{(1,2)} = \left[\Omega \mp \sqrt{\Omega^2 - 4}\right] \Big/ 2, \tag{6}$$

$$\Omega = \left[\left(1 + S_{11}^{(1)}\right)^2 S_{11}^{(2)} - \left(1 - S_{11}^{(1)}\right)^2 + 2\left(1 - S_{11}^{(2)}\right)\right] \Big/ \left(S_{11}^{(1)2} + S_{11}^{(2)}\right). \tag{7}$$

Once determining Γ from Eqs. (6) and (7), T_1, T_2, ε_r, and μ_r can be found as

$$T_u = \sqrt{\left(\Gamma - S_{11}^{(u)}\right) \Big/ \left(1 - \Gamma S_{11}^{(u)}\right)}, \ 1/\Lambda = i \ln\left(T_u\right)/(2\pi L_u), \tag{8}$$

$$\mu_r = \frac{\lambda_0}{\sqrt{1 - (\lambda_0/\lambda_c)^2}} \frac{1}{\Lambda} \left(\frac{1 + \Gamma}{1 - \Gamma}\right), \ \varepsilon_r = \frac{\lambda_0^2}{\mu_r} \left(\frac{1}{\Lambda^2} + \frac{1}{\lambda_c^2}\right), \tag{9}$$

$$\ln\left(T_u\right) = \ln\left(|T_u|\right) + i(\phi_u \mp 2\pi m_u), \ m_u = 0, 1, 2, \ldots \tag{10}$$

Since the complex guided wavelength Λ relates to the sample propagation constant γ in the complex propagation factors T_1 and T_2 in Eq. (8), unique solutions for ε_r and μ_r are generally not possible from Eq. (9). This is because correct assignment of m_u integer values in the argument of complex wavenumber is required for the correct retrieval of
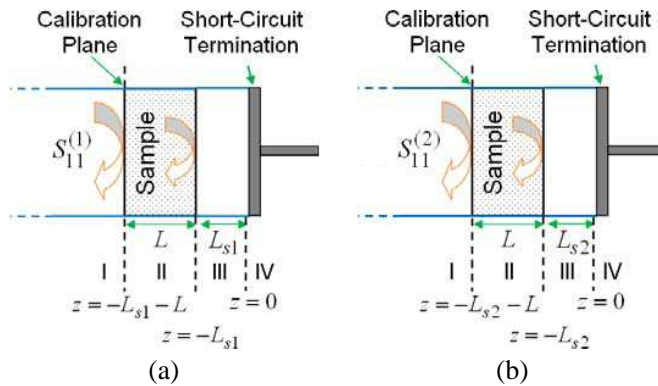
ε_r and μ_r. By using the phase unwrapping technique, which exploits the continuity of the guided wavelength over frequency [28], unique solution for ε_r and μ_r will be cast as discussed in the following section.

Although the technique of using two identical samples with different lengths is effective in measuring the ε_r and μ_r parameters of materials, any impurity and/or inhomogeneity present in the second sample may drastically lower the accuracy of measurements. In addition, using two samples increase the overall thickness uncertainty [37]. In the next subsection, we propose another reflection-only measurement configuration for eliminating the preceding drawbacks.

2.2. Measurements of One Sample with a Variable Short-circuit

To eliminate the problems of reflection-only measurements of two identical samples, here, we propose another measurement configuration based on reflection-only measurements of one sample with non-flushing two short-circuit terminations, L_{s1} and L_{s2}, as shown in Fig. 2. In this configuration, the sample is positioned into the waveguide section and varying the location of termination, independent reflection-only measurements are carried out for retrieving ε_r and μ_r of the sample.

As in the case of reflection-only measurements of two identical samples, assuming the sample is a simple medium and only the dominant mode (TE_{10}^z) is propagating through the sample, electric

Figure 2. Measurement configuration for constitutive parameters retrieval from shifted short-circuit measurements through the phase unwrapping technique.

vector potential, $\vec{F}$, for regions I, II, and III as can be written

$$F_z^{(I)}(x,z) = \psi(x)\left[C_5 e^{-\gamma_0 z} + C_6 e^{\gamma_0 z}\right], \tag{11}$$

$$F_z^{(II)}(x,z) = \psi(x)\left[C_7 e^{-\gamma z} + C_8 e^{\gamma z}\right], \tag{12}$$

$$F_z^{(III)}(x,z) = \psi(x)\left[C_9 e^{-\gamma_0 z} + C_{10} e^{\gamma_0 z}\right], \tag{13}$$

Here, C_5 : C_{10} are complex amplitudes, and the definitions and expressions of each variable in Eqs. (11)–(13) have the same meaning and usage as in Subsection 2.1. Applying boundary conditions (continuation of tangential components of electric and magnetic fields and vanishing of tangential electric field at the short-circuit termination (PEC) at interfaces I-II, II-III, and III-IV ($z = 0$, $z = -L_{s1}$ or $z = -L_{s2}$, and $z = -L - L_{s1}$ or $z = -L - L_{s2}$), S_{11} at the calibration plane can be derived as

$$S_{11}^{(u)} = \frac{\Gamma\left(1 - T^2\right) + \left(\Gamma^2 - T^2\right)T_{su}^2}{\left(1 - \Gamma^2 T^2\right) + \Gamma\left(1 - T^2\right)T_{su}^2}, \tag{14}$$

where γ and Γ are given in Eqs. (3) and (4), and $T_{su} = \exp\left(-\gamma_0 L_{su}\right)$. Here, L_{s1} and L_{s2}, the distances between the sample back surface and the front face of short-circuit termination, are assumed to be known precisely. Performing reflection-only measurements for two different positions of the variable termination, L_{s1} and L_{s2} in Fig. 2, we can eliminate T^2 terms in Eq. (14) and derive

$$\Gamma_{(1,2)} = \left(-\Omega_2 \mp \sqrt{\Omega_2^2 - 4\Omega_1^2}\right)\Big/2\Omega_1, \tag{15}$$

$$\Omega_1 = T_{s1}^2 S_{11}^{(2)} - T_{s2}^2 S_{11}^{(1)}, \tag{16}$$

$$\Omega_2 = S_{11}^{(2)} - S_{11}^{(1)} + T_{s2}^2 - T_{s1}^2 + T_{s2}^2 S_{11}^{(2)}\left(S_{11}^{(1)} + T_{s1}^2\right) - T_{s1}^2 S_{11}^{(1)}\left(S_{11}^{(2)} + T_{s2}^2\right). \tag{17}$$

The correct choice for Γ in Eq. (15) can be found using $\left|\Gamma_{(1,2)}\right| \leq 1$, as discussed in Subsection 2.1. After determining the correct Γ, T can be computed by

$$T = \sqrt{\frac{\left(1 + T_{su}^2 \Gamma\right)\left(\Gamma - S_{11}^{(u)}\right)}{\left(\Gamma + T_{su}^2\right)\left(1 - \Gamma S_{11}^{(u)}\right)}}. \tag{18}$$

Finally, ε_r and μ_r can be found from Eq. (9). We note that, in this measurement configuration, we could have assumed either $L_{s1} = 0$ or $L_{s2} = 0$ to simplify the analysis. However, here, we have tried to keep our analysis as general as possible. Although the shifted short-circuited measurements eliminate errors arising from using the second sample, they require the knowledge of L_{s1} and L_{s2}. As

pointed out in Subsection 2.1, the correct assignment of m_u integer values in the argument of complex wavenumber is a requirement for correct retrieval of constitutive parameters. In the next section, we will discuss the phase unwrapping technique for retrieving correct constitutive parameters for two reflection-only (one-port) measurement configurations analyzed in this section.

3. PHASE UNWRAPPING METHOD

In this section, we apply the phase unwrapping technique for retrieval of ε_r and μ_r of samples using reflection-only measurements mentioned in previous section.
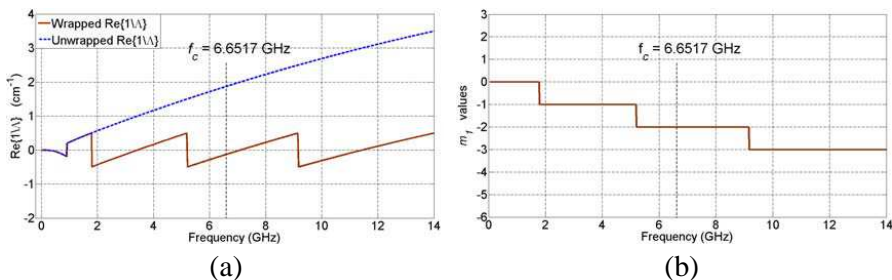
3.1. Two Sample Measurements

For validation of the phase unwrapping technique for two sample short-circuited measurements in Fig. 1, we first assume some test constitutive parameters and sample lengths to calculate Γ and T, then substitute them into Eq. (4) to determine S_{11} values, and finally retrieve the parameters using the proposed technique. For example, we use the distilled water at 30°C as the test sample whose dielectric properties can be analytically estimated by the Debye model [38] as

$$\varepsilon_r(\omega) = \varepsilon_\infty + (\varepsilon_s - \varepsilon_\infty)/(1 + i\omega\tau). \qquad (19)$$

Here, ε_∞ is the so-called infinite frequency permittivity, ε_s the static value (DC value) of the permittivity, and τ the relaxation time. Setting $\varepsilon_\infty = 4.9$, $\varepsilon_s = 76.47$, and $\tau = 7.2\,\text{ps}$, we see in Fig. 3(a) that the principal absorption band (interpreted as being due to a relaxation of molecular origin) shows a maximum at around 22.1 GHz. Next
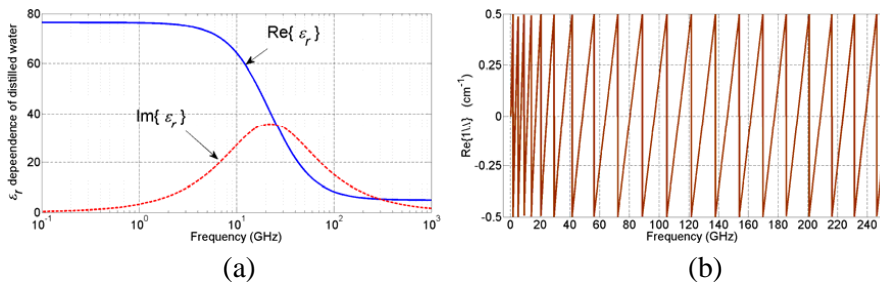
Figure 3. (a) Dependence of permittivity of distilled water over f and (b) real part of inverse of the wrapped complex guided wavelength using two sample measurements ($L_1 = 1.0\,\text{cm}$).

Figure 4. (a) Wrapped (continuous line) and unwrapped (dashed line) real part of complex guided wavelength for the 1.0-cm thick sample using two-sample measurements, and (b) dependence of m_1 values over frequency to obtain unwrapped Re $\{1/\Lambda\}$ dependence in Fig. 4(a) using two sample short-circuit measurements.

we assume $\mu_r = 1.0 - i0.7$ for the magnetic permeability of distilled water and choose $L_1 = 1.0$ cm and $L_2 = 2.0$ cm for the sample lengths, $f_c = 6.6517$ GHz, and this completes the input data for the calculation of the S-parameters from Eq. (4). Note that we utilize a μ_r value different than that used in [28] to test the phase unwrapping technique for various constitutive parameter combinations.

Substituting $S_{11}^{(1)}$ and $S_{11}^{(2)}$ into Eqs. (6) and (7), we first determine Γ. Then, we put its value into Eq. (8) for obtaining T_1 and T_2. After, using Eq. (8), we draw Re $\{1/\Lambda\}$, as shown in Fig. 3(b) without the application of the phase unwrapping technique. From the dependence in Fig. 3(b), we note that the thickness of the sample can be extracted from the bouncing off nature of Re $\{1/\Lambda\}$ over frequency between $+\pi$ and $-\pi$ [28]. It was observed in [28] a negative slope of the sawtooth waveform of Re $\{1/\Lambda\}$ before the cutoff frequency, and a positive slope after the cutoff frequency. Here, we have a different scenario. Inclusion of magnetic loss ($\tan \delta_m = 0.7$) into simulation changes the slope pattern of Re $\{1/\Lambda\}$ before cutoff frequency. This is seen in greater detail for the dependence of wrapped Re $\{1/\Lambda\}$ (continuous line) over the range 0–14 GHz in Fig. 4(a). In the same figure, the unwrapped Re $\{1/\Lambda\}$ (dashed line) is superposed over the wrapped one. In obtaining the unwrapped Re $\{1/\Lambda\}$ in Fig. 4(a), correct integer values of m_u in Eq. (10) are assigned to obtain a continuous dependence, corresponding to adding a phase function to the inverse of the complex wavelength, $1/\Lambda$ [28], by

$$\lim_{\phi_u \to \pm \pi} f\left(\phi_u\right) = f\left(\pm \pi\right), \quad \mid f\left(\phi_u\right) - f\left(\pm \pi\right)\mid < \delta_1, \quad \mid \phi_u - \left(\pm \pi\right) \mid < \delta_2, \quad (20)$$

where $f\left(\phi_u\right) = \text{Re}\{1/\Lambda\}$ and δ_1 and δ_2 are the small positive numbers.
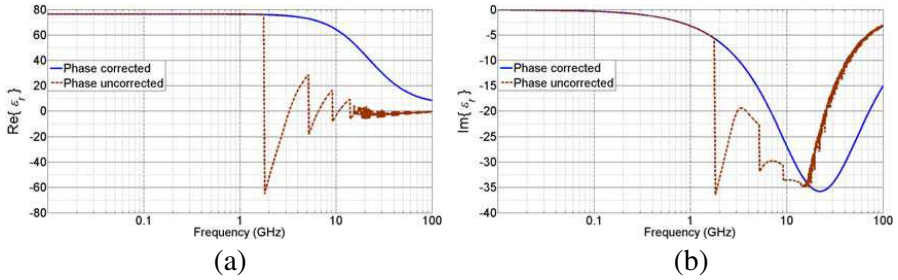
Figure 5. Retrieved (a) real part and (b) imaginary part of the ε_r using two sample measurements for corrected and uncorrected phases from Eqs. (5)–(10).
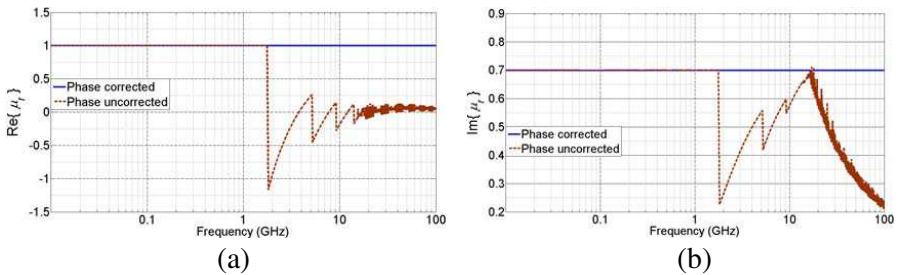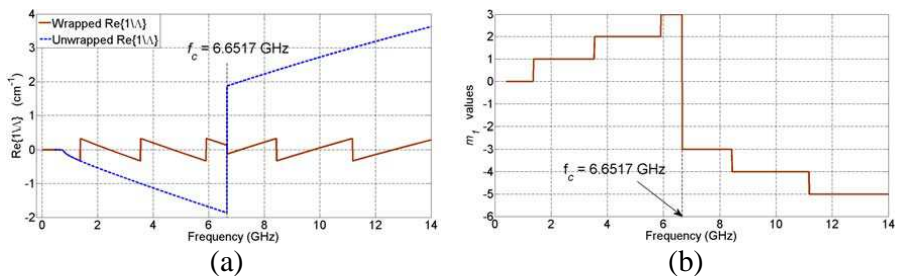

Figure 6. Retrieved (a) real part and (b) imaginary part of the μ_r using two sample measurements for corrected and uncorrected phases from Eqs. (5)–(10).

This approach also resembles to Riemann surfaces in complex variables used for keeping a multi-valued function as single-valued. The assigned values of m_1 to have continuous dependence of Re $\{1/\Lambda\}$ using Eq. (20) are shown in Fig. 4(b). It is seen from Fig. 4(b) that we have dependence of m_1 values different than that in Fig. 5 of [28]. This difference arises as a consequence of the inclusion of $\tan \delta_m$. Whenever electrical properties and the sample lengths change, the dependencies in Figs. 3(b)–4(b) change since T_1 and T_2 in Eq. (4) are both functions of ε_r, μ_r, and L_1 (or L_2). Once the real part of complex wavelength Λ is unwrapped, then we proceed to retrieve the parameters ε_r and μ_r. Following the proposed unwrapping procedure, retrieved ε_r and μ_r of water are shown in Figs. 5 and 6, respectively. Upon comparison with the Debye representation (Fig. 3(a)), it is clearly apparent that real and imaginary parts of ε_r are correctly retrieved. The same is valid for the retrieved μ_r and assumed μ_r ($= 1.0 - i0.7$). In Fig. 5(a) through Fig. 6(b), the components of permittivity and permeability extracted for the unwrapping case are also indicated by dashed lines.
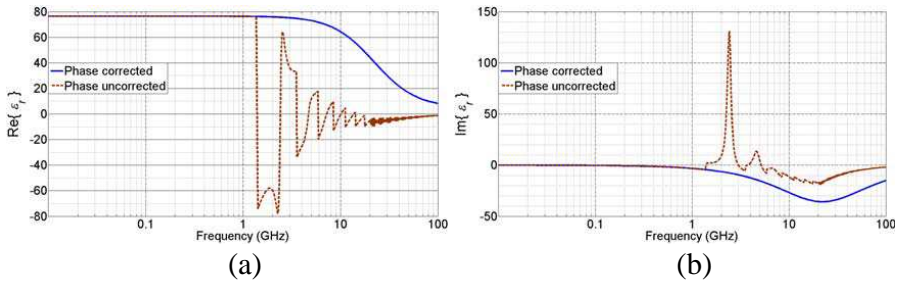
3.2. Shifted Short-circuit Measurements

We use, as before, distilled water whose frequency-dependent ε_r is shown in Fig. 3(a), as our test sample for illustration of the phase unwrapping technique for shifted short-circuit reflection measurements of one sample (Fig. 2). This time, we assume $\mu = 1.0 - i0.0$ for the magnetic permeability of distilled water and choose $L = 1.5\,\text{cm}$ for the sample length, $L_{s1} = 2\,\text{mm}$ and $L_{s2} = 3\,\text{mm}$ for the distance between back surface and the shifted short-circuit termination, $f_c = 6.6517\,\text{GHz}$, and this completes the input data for the calculation of the S-parameters from Eq. (14). Substituting these calculated $S_{11}^{(1)}$ and $S_{11}^{(2)}$ into Eqs. (15)–(17), we first determine Γ using the constraint $|\Gamma| \leq 1$. Then, we put its value into Eq. (18) for obtaining T. After, using Eq. (8), we obtain the dependence of $\text{Re}\{1/\Lambda\}$ over frequency. We note that the thickness of the sample can be extracted from the bouncing off nature of $\text{Re}\{1/\Lambda\}$ over frequency (Fig. 7(a)) when its value approaches $1/3.0\,\text{cm}^{-1}$, yielding a sample thickness of $L = 1.5\,\text{cm}$.

To obtain a continuous dependence of $\text{Re}\{1/\Lambda\}$ on frequency, using Eq. (20), we unwrap it and attain the dependence in Fig. 7(a) for a frequency range 0–14 GHz to see in great detail. In obtaining a continuous dependence for $\text{Re}\{1/\Lambda\}$ over a broad frequency band, we consider two distinct regions as $f < f_c$ and $f > f_c$ [28], as can be seen from negative slope of $\text{Re}\{1/\Lambda\}$ before cutoff frequency, and then positive slope of $\text{Re}\{1/\Lambda\}$ after cutoff frequency in Fig. 7(a). Continuous dependence corresponds to adding a piecewise phase function to the inverse of the complex wavelength, $1/\Lambda$ [28]. The

Figure 7. (a) Wrapped (continuous line) and unwrapped (dashed line) real part of complex guided wavelength for the 1.5-cm thick sample using shifted short-circuit measurements and (b) dependence of m_1 values over frequency to obtain unwrapped $\text{Re}\{1/\Lambda\}$ dependence in Fig. 7(a) using shifted short-circuit measurements.

Figure 8. Retrieved (a) real part and (b) imaginary part of the ε_r using shifted short-circuit measurements for corrected and uncorrected phases from Eqs. (15)–(18).
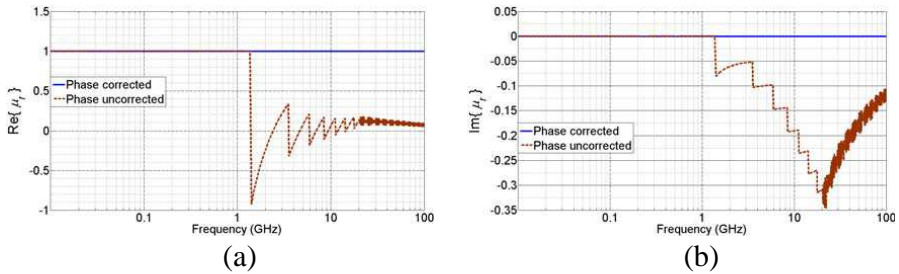
Figure 9. Retrieved (a) real part and (b) imaginary part of the μ_r using shifted short-circuit measurements for corrected and uncorrected phases from Eqs. (15)–(18).

assigned values of m_1 to have continuous dependence of $\mathrm{Re}\{1/\Lambda\}$ are shown in Fig. 7(b). Comparing the dependencies in Figs. 4(a) (or 4(b)) and 7(a) (or 7(b)), we note that although we should consider the regions before and after the cutoff frequency as two separate regions, in some cases, at cutoff frequency, continuity of $\mathrm{Re}\{1/\Lambda\}$ may assure that the values of $\mathrm{Re}\{1/\Lambda\}$ at immediately before and immediately after the cutoff frequency are equal in magnitude $(1.83\,\mathrm{cm}^{-1})$ (Fig. 4(a)). This circumstance, sometimes, arise for some combinations of thickness and electrical properties of the sample.

After unwrapping the complex wavelength, we continue to retrieve the parameters ε_r and μ_r. Following the proposed unwrapping procedure, retrieved ε_r and μ_r of water are shown in Figs. 8 and 9, respectively. As before, upon comparison with the Debye representation (Fig. 3(a)), it is clearly apparent from Fig. 8 that real and imaginary parts of ε_r are correctly retrieved. The same is valid for the retrieved μ_r and assumed $\mu_r \, (= 1.0 - i0.0)$. In Figs. 8 and 9, the components of ε_r and μ_r extracted for the unwrapping case are also indicated by dashed lines.

4. CONCLUSIONS

We applied the phase unwrapping method as a powerful tool to solve the phase ambiguity problem posed by the multiple-valued logarithm function of the complex transmission coefficient in the scattering equations of reflection-only (one-port) measurements, since at some instances, only the front face of the specimen is visible to incident electromagnetic radiation. We considered two special cases for testing the method. In the first case, reflection scattering parameter measurements of two identical samples shorted by a short-circuit termination (samples back faces and termination are flushed) are utilized and then the phase unwrapping method is applied. In the second case, reflection scattering parameter measurements of one sample shorted by a varying short-circuit termination are used and afterwards the phase unwrapping method is implemented. We accurately retrieved the electromagnetic properties of distilled water used as a test sample using phase unwrapping method for the preceding two measurement configurations. For both configurations, we note that the continuity of complex wavelength is the core feature of the phase unwrapping technique, that for some combinations of sample electromagnetic properties and lengths, real part of the complex wavelength does not necessarily abruptly changes its value at cutoff frequency, and that the sample length, which is a prerequisite in some methods, can be extracted directly from dependence of the real part of the complex wavelength using reflection-only measurements.

REFERENCES

1. Zhang, H., S. Y. Tan, and H. S. Tan, "An improved method for microwave nondestructive dielectric measurement of layered media," *Progress In Electromagnetics Research B*, Vol. 10, 145–161, 2008.

2. Bombay, M. S. and O. M. Ramahi, "Near-field probes using double and single negative media," *Phys. Rev. E*, Vol. 79, 016602, 2009.

3. Hasar, U. C., "Permittivity determination of fresh cement-based materials by an open-ended waveguide probe using amplitude-only measurements," *Progress In Electromagnetics Research*, Vol. 97, 27–43, 2009.

4. Nicolson, A. M. and G. F. Ross, "Measurement of the intrinsic properties of materials by time-domain," *IEEE Trans. Instrum. Meas.*, Vol. 19, No. 4, 377–382, 1970.

5. Hyde, IV, M. W. and M. J. Havrilla, "A nondestructive technique for determining complex permittivity and permeability

of magnetic sheet materials using two flanged rectangular waveguides," *Progress In Electromagnetics Research*, Vol. 79, 367–386, 2008.

6. Hasar, U. C. and I. Y. Ozbek, "Complex permittivity determination of lossy materials at millimeter and terahertz frequencies using free-space amplitude measurements," *Journal of Electromagnetic Waves and Applications*, Vol. 25, Nos. 14–15, 2100–2109, 2011.

7. Ho, M., "Penetration of EM fields into circular dielectric/magnetic container: Two-dimensional simulation," *Journal of Electromagnetic Waves and Applications*, Vol. 25, No. 1, 111–122, 2011.

8. Moradi, G. and A. Abdipour, "Measuring the permittivity of dielectric materials using STDR approach." *Progress In Electromagnetics Research*, Vol. 77, 357–365, 2007.

9. Yan, L. P., K.-M. Huang, and C. J. Liu, "A noninvasive method for determining dielectric properties of layered tissues on human back," *Journal of Electromagnetic Waves and Applications*, Vol. 21, No. 13, 1829–1843, 2007.

10. Boughriet, A. -H., C. Legrand, and A. Chapoton, "A noniterative stable transmission/reflection method for low-loss material complex permittivity determination," *IEEE Trans. Microw. Theory Tech.*, Vol. 45, No. 1, 52–57, 1997.

11. Wang, Y. and M. N. Afsar, "Measurement of complex permittivity of liquids using waveguide techniques," *Progress In Electromagnetics Research*, Vol. 42, 131–142, 2003.

12. Stuchly, S. S. and M. Matuszewski, "A combined total reflection transmission method in application to dielectric spectroscopy," *IEEE Trans. Instrum. Meas.*, Vol. 27, No. 3, 285–288, 1978.

13. Seal, M. D., M. W. Hyde, and M. J. Havrilla, "Nondestructive complex permittivity and permeability extraction using a two-layer dual-waveguide probe measurement geometry," *Progress In Electromagnetics Research*, Vol. 123, 123–142, 2012.

14. Baker-Jarvis, J., E. J. Vanzura, and W. A. Kissick, "Improved technique for determining complex permittivity with the transmission/reflection method," *IEEE Trans. Microw. Theory Tech.*, Vol. 38, No. 8, 1096–1103, 1990.

15. Ghodgaonkar, D. K., V. V. Varadan, and V. K. Varadan, "A free-space measurement of complex permittivity and complex permeability of magnetic materials at microwave frequencies," *IEEE Trans. Instrum. Meas.*, Vol. 39, No. 2, 387–394, 1990.

16. Muqaibel, A. H. and A. Safaai-Jazi, "A new formulation for characterization of materials based on measured insertion transfer function," *IEEE Trans. Microw. Theory Tech.*, Vol. 51, No. 8, 1946–1951, 2003.

17. Weir, W. B., "Automatic measurement of complex dielectric constant and permeability at microwave frequencies," *Proc. IEEE*, Vol. 62, No. 1, 33–36, 1974.

18. Ness, J., "Broad-band permittivity measurements using the semi-automatic network analyzer," *IEEE Trans. Microw. Theory Tech.*, Vol. 33, No. 11, 1222–1226, 1985.

19. Ball, J. A. R. and B. Horsfield, "Resolving ambiguity in broadband waveguide permittivity measurements on moist materials," *IEEE Trans. Instrum. Meas.*, Vol. 47, No. 2, 390–392, 1998.

20. Hasar, U. C. and O. E. Inan, "Elimination of the multiple-solutions ambiguity in permittivity extraction from transmission-only measurements of lossy materials," *Microw. Opt. Technol. Lett.*, Vol. 51, No. 2, 337–341, 2009.

21. Xia, S., Z. Xu, and X. Wei, "Thickness-induced resonance-based complex permittivity measurement technique for barium strontium titanate ceramics at microwave frequency," *Rev. Sci. Instrum.*, Vol. 80, No. 11, 114703, 2009.

22. Hasar, U. C., "Unique permittivity determination of low-loss dielectric materials from transmission measurements at microwave frequencies," *Progress In Electromagnetics Research*, Vol. 107, 31–46, 2010.

23. Hasar, U. C., "Unique retrieval of complex permittivity of low-loss dielectric materials from transmission-only measurements," *IEEE Geosci. Remote Sens. Lett.*, Vol. 8, No. 3, 562–564 2011.

24. Chen, X., T. M. Gregorczyk, B.-I. Wu, J. Pacheco, Jr., and J. A. Kong, "Robust method to retrieve the constitutive effective parameters of metamaterials," *Phys. Rev. E*, Vol. 70, 016608, 2004.

25. Buyukozturk, O., T-Y. Yu, and J. A. Ortega, "A methodology for determining complex permittivity of construction materials based on transmission-only coherent, wide-bandwidth free-space measurements," *Cem. Concr. Compos.*, Vol. 28, 349–359, 2006.

26. Varadan, V. V. and R. Ro, "Unique retrieval of complex permittivity and permeability of dispersive materials from reflection and transmitted fields by enforcing causality," *IEEE Trans. Microw. Theory Tech.*, Vol. 55, No. 10, 2224–2230, 2007.

27. Szabó, Z., G.-H. Park, R. Hedge, and E.-P. Li, "A unique extraction of metamaterial parameters based on Kramers-Kronig relationship," *IEEE Trans. Microw. Theory Tech.*, Vol. 58, No. 10, 2646–2653, 2010.

28. Barroso, J. J. and U. C. Hasar, "Resolving phase ambiguity in the inverse problem of transmission/reflection measurement methods," *J. Infrared Milli. Terahz Waves*, Vol. 32, 857–866, 2011.

29. Chavez, S., Q.-S. Xiang, and L. An, "Understanding phase maps in MRI: A new cutline phase unwrapping method," *IEEE Trans. Med. Imag.*, Vol. 21, No. 8, 966–977, 2002.

30. Huang, Y., "Design, calibration and data interpretation of a one-port large coaxial dielectric measurement cell," *Meas. Sci. Technol.*, Vol. 12, 111–115, 2001.

31. Hasar, U. C. and M. T. Yurtcan, "A microwave method based on amplitude-only reflection measurements for permittivity determination of low-loss materials," *Measurement*, Vol. 43, No. 9, 1255–1265, 2010.

32. Balanis, C. A., *Advanced Engineering Electromagnetics*, Wiley, West Sussex, NJ, 2012.

33. Baker-Jarvis, J., M. D. Janezic, J. H. Grosvenor, Jr., and R. G. Geyer, "Transmission/reflection and short-circuit line methods for measuring permittivity and permeability," Tech. Note 1355, NIST, Boulder, CO, 1992.

34. Landau, L. D., E. M. Lifshitz, and L. P. Pitaevskii, *Electrodynamics of Continuous Media*, 279, Pergamon, Oxford, 1984.

35. Woodly, J. and M. Mojahedi, "On the signs of the imaginary parts of the effective permittivity and permeability in metamaterials," *J. Opt. Soc. Am. B.*, Vol. 27, No. 5, 1016–1021, 2010.

36. Wang, H., X. Chen, and K. Huang, "An improved approach to determine the branch index for retrieving the constitutive effective parameters of metamaterials," *Journal of Electromagnetic Waves and Applications*, Vol. 25, No. 1, 85–96, 2011.

37. Hasar, U. C., "A new calibration-independent method for complex permittivity extraction of solid materials," *IEEE Microw. Wireless Compon. Lett.*, Vol. 18, No. 12, 788–790, 2008.

38. Ellison, W. J., K. Lamkaouchi, and J.-M. Moreau, "Water: A dielectric reference," *J. Mol. Liq.*, Vol. 68, Nos. 2–3, 171–279, 1996.